

Analysis of the Rubberband Algorithm

Fajie Li and Reinhard Klette

Computer Science Department and CITR, The University of Auckland
Auckland, New Zealand

Abstract. We consider simple cube-curves in the orthogonal 3D grid of cells. The union of all cells contained in such a curve (also called the tube of this curve) is a polyhedrally bounded set. The curve's length is defined to be that of the minimum-length polygonal curve (MLP) contained and complete in the tube of the curve. Only one general algorithm, called rubberband algorithm, was known for the approximative calculation of such an MLP so far.

An open problem in [7] is related to the design of algorithms for the calculation of the MLP of a simple cube-curve: Is there a simple cube-curve such that none of the nodes of its MLP is a grid vertex? This paper constructs an example of such a simple cube-curve, and we also characterize the class of all of such cube-curves. This study leads to a correction in Option 3 of the rubberband algorithm (by adding one missing test).

We also prove that the rubberband algorithm has linear time complexity $\mathcal{O}(m)$ where m is the number of critical edges of a given simple cube curve, which solves another open problem in the context of this algorithm.

1 Introduction

The analysis of cube-curves is related to (e.g.) path planning in a cuboidal world of robots, or length estimation in 3D image analysis; for recent applications of the rubberband algorithm of [1] in 3D medical imaging, see, for example, [4, 13].

A cube-curve can be seen as the result of a digitization process which maps a curve-like object into a union S of face-connected closed cubes. The length of a simple cube-curve S in 3D Euclidean space can be defined by the (Euclidean) length of the **minimum-length polygonal curve** (MLP for short) contained and complete in the polyhedrally bounded compact set S [10, 11].

1.1 Related Work

The computation of the length of a simple cube-curve in 3D Euclidean space was a subject in [5]; the proposed method is based on adding weights of local steps. [1] presents an algorithm (there called the *rubberband algorithm*) for computing an approximate MLP in S with measured time complexity in $\mathcal{O}(n)$, where n is the number of grid cubes of the given cube-curve. The rubberband algorithm is

not based on local weights, rather on an iterative scheme for optimizing positions of nodes of polygonal curves, supposed to converge against the MLP. We refer to [1] or to Section 11.1.4 in [7] for a detailed description of the rubberband algorithm, and for its iteration steps see Appendix 1.

The difficulty of the computation of the MLP in 3D may be illustrated by the fact that the Euclidean shortest path problem (i.e., find a shortest obstacle-avoiding path from source point to target point, for a given finite collection of polyhedral obstacles in 3D space, a source, and a target point) is known to be NP-hard [2]. However, there are some algorithms solving the approximate Euclidean shortest path problem in 3D with polynomial-time, see [3]. So far it is not yet shown whether the rubberband algorithm is always convergent towards the correct MLP, or not (i.e., so far never a provable incorrect result has been obtained).

Recently, [8] developed a polynomial-time algorithm for the calculation of MLPs which is provable correct for a special class of simple cube-curves. The main idea is to decompose a simple cube-curve into some kinds of arcs by finding “end angles” (see Definition 4 below) in the given simple cube-curve.

There is an open problem (see [7, page 406]) which is related to the design of algorithms for the calculation of the MLP of a simple cube-curve: Is there a simple cube-curve such that none of the nodes of its MLP is a grid vertex? This paper constructs an example of such a simple cube-curve, and generalizes this by characterizing the class of all of those cube-curves. Cube-curves in this class do not have any end angle; this means that we cannot use the MLP algorithm proposed in [8] which is provable correct. This is the basic importance of the given result: we show the existence of cube-curves which require further algorithmic studies, in particular the question whether the (corrected) rubberband algorithm always generates a unique spatial polygon or not.

1.2 Notations and Definitions

Following [1, 6], a grid point $(i, j, k) \in \mathbb{Z}^3$ is assumed to be the center point of a *grid cube* with *faces* parallel to the coordinate planes, with *edges* of length 1, and *vertices* as its corners. *Cells* are either cubes, faces, edges, or vertices. The intersection of two cells is either empty or a joint *side* of both cells. A *cube-curve* is an alternating sequence $g = (f_0, c_0, f_1, c_1, \dots, f_n, c_n)$ of faces f_i and cubes c_i , for $0 \leq i \leq n$, such that faces f_i and f_{i+1} are sides of cube c_i , for $0 \leq i \leq n$ and $f_{n+1} = f_0$. It is *simple* iff $n \geq 4$ and for any two cubes $c_i, c_k \in g$ with $|i - k| \geq 2 \pmod{n+1}$, if $c_i \cap c_k \neq \emptyset$ then either $|i - k| = 2 \pmod{n+1}$ and $c_i \cap c_k$ is an edge, or $|i - k| \geq 3 \pmod{n+1}$ and $c_i \cap c_k$ is a vertex.

A *simple cube-arc* is an alternating sequence $a = (f_0, c_0, f_1, c_1, \dots, f_k, c_k)$ of faces f_i and cubes c_i with $f_k \neq f_0$, denoted by $a = (c_0, c_1, \dots, c_k)$ or $a(c_0, c_k)$ for short, which is a proper subsequence of a simple cube-curve. A *subarc* of an arc $a = (c_0, c_1, \dots, c_k)$ is an arc $(c_i, c_{i+1}, \dots, c_j)$, where $0 \leq i \leq j \leq k$.

We recall a few basic definitions from the book [7] (page 312). A (finite) *word* defined over an alphabet A is a finite sequence of elements of A . The *length* $|u|$ of the word $u = b_1 b_2 \dots b_n$ (where each $b_i \in A$) is the number n of *letters* b_i

in u . An integer $k \leq 1$ is a *period* of a word $u = b_1b_2 \dots b_n$ if $b_i = b_{i+k}$, for $i = 1, \dots, n - k$. The smallest period of u is called *the* period of u . A finite word u is *periodic* if the period of u is less than the length of u . A finite word u is *aperiodic* if u is not periodic.

A simple cube-arc $a = (c_0, c_1, \dots, c_k)$ can correspond to a word over the alphabet $\{1,2,3,4,5,6\}$ as follows: A single cube c_0 corresponds to the empty word. If c_1 is on the front (back, right, left, top, or bottom) of c_0 , then c_1 corresponds to 1 (2, 3, 4, 5, or 6). The other cubes of a define corresponding numbers in the same way, encoding the direction from the previous cube. The resulting word is called the *word of a* . A simple cube-arc a is *periodic* iff its resulting word is periodic. a is *aperiodic* iff its resulting word is aperiodic.

In this paper, all cube-arcs are simple cube-arcs.

A *tube \mathbf{g}* is the union of all cubes contained in a cube-curve g . A tube is a compact set in \mathbb{R}^3 , its frontier defines a polyhedron. A curve in \mathbb{R}^3 is *complete* in \mathbf{g} iff it has a nonempty intersection with every cube contained in g . Following [6, 10, 11], we define:

Definition 1. *An approximating minimum-length curve of a simple cube-curve g is a shortest simple curve P which is contained and complete in tube \mathbf{g} . The length of a simple cube-curve g is defined to be the length $l(P)$.*

It turns out that such a shortest simple curve P is always a polygonal curve, called a *minimum-length polygon (MLP)*, and it is uniquely defined if the cube-curve is not only contained in a single layer of cubes of the 3D grid (see [10, 11]). If it is contained in one layer, then the MLP is uniquely defined up to a translation orthogonal to that layer. We speak about *the* MLP of a simple cube-curve.

A *critical edge* of a cube-curve g is such a grid edge which is incident with exactly three different cubes contained in g . Figure 1 shows all the critical edges of a simple cube-curve.

Definition 2. *If e is a critical edge of g and l is a straight line such that $e \subset l$, then l is called the critical line of e in g , or a critical line for short.*

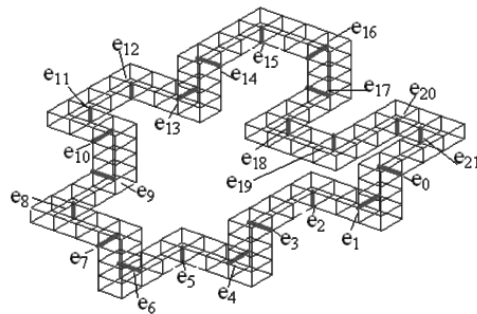


Fig. 1. Example of a first-class simple cube-curve which has both inner and end angles.

Definition 3. Let e be a critical edge of g . Let P_1 and P_2 be the two end points of e (i.e., they only differ in one coordinate). If one of the coordinates of P_1 is less than the corresponding coordinate of P_2 , then P_1 is called the first end point of e , otherwise P_1 is called the second end point of e .

Definition 4. Assume a simple cube-curve g and a triple of consecutive critical edges e_1, e_2 , and e_3 such that $e_i \perp e_j$, for all $i, j = 1, 2, 3$ with $i \neq j$. If e_2 is parallel to the x -axis (y -axis, or z -axis) and the x -coordinates (y -coordinates, or z -coordinates) of two end points of e_1 and e_3 are equal, then we say that e_1, e_2 and e_3 form an end angle, and g has an end angle, denoted by $\angle(e_1, e_2, e_3)$; otherwise we say that e_1, e_2 and e_3 form an inner angle, and g has an inner angle.

Figure 1 shows a simple cube-curve which has five end angles $\angle(e_{21}, e_0, e_1)$, $\angle(e_4, e_5, e_6)$, $\angle(e_6, e_7, e_8)$, $\angle(e_{14}, e_{15}, e_{16})$, $\angle(e_{16}, e_{17}, e_{18})$, and many inner angles (e.g., $\angle(e_0, e_1, e_2)$, $\angle(e_1, e_2, e_3)$, or $\angle(e_2, e_3, e_4)$).

Let $S \subseteq \mathbb{R}^3$. The set $\{(x, y, 0) : \exists z(z \in \mathbb{R} \wedge (x, y, z) \in S)\}$ is the xy -projection of S , or *projection* of S for short. Analogously we have the yz - or xz -projection of S .

Let e_1, e_2, \dots, e_m be a subsequence of all consecutive critical edges $\dots, e_0, e_1, \dots, e_m, e_{m+1}, \dots$ of a cube-curve g . Let $m \geq 2$.

Definition 5. If $e_0 \perp e_1$, $e_m \perp e_{m+1}$, and $e_i \parallel e_{i+1}$, where $i = 1, 2, \dots, m-1$, then e_1, e_2, \dots, e_m is a maximal run of parallel critical edges of g , and critical edges e_0 or e_{m+1} are called adjacent to this run.

Figure 1 shows a simple cube-curve which has two maximal runs of parallel critical edges: e_{11}, e_{12} and $e_{18}, e_{19}, e_{20}, e_{21}$. The two adjacent critical edges of run e_{11}, e_{12} are e_{10} and e_{13} ; they are on two different grid planes. The two adjacent critical edges of run $e_{18}, e_{19}, e_{20}, e_{21}$ are e_{17} and e_0 ; they are also on two different grid planes.

1.3 First-Class Simple Cube Curves; Structure of Paper

Definition 6. A simple cube-curve g is called first-class iff each critical edge of g contains exactly one vertex of the MLP of g .

This paper focuses on first-class simple cube-curves,¹ and general simple cube-curves require further studies.

The paper is organized as follows. Section 2 describes theoretical fundamentals for constructing our example in Section 4 where non of the nodes of the MLP is a grid vertex. Section 2 also proves that the rubberband algorithm has linear time complexity $\mathcal{O}(m)$, where m is the number of critical edges of a given simple cube curve. Section 2 also presents theoretical fundamentals for Section 5. Section 5 improves the original rubberband algorithm in its Option 3. Section 6 gives a few conclusions.

¹ We can classify a simple cube-curve to be first class or not by running the rubberband algorithm as described in [1]: the curve is first class iff option (O_1) does not occur.

2 Theoretical Results

We start with citing a basic theorem from [6]:

Theorem 1. *Let g be a simple cube-curve. Critical edges are the only possible locations of vertices of the MLP of g .*

Let $d_e(p, q)$ be the Euclidean distance between points p and q .

2.1 Theorem on Endangles

Let $e_0, e_1, e_2, \dots, e_m$ and e_{m+1} be $m + 2$ consecutive critical edges in a simple cube-curve, and let $l_0, l_1, l_2, \dots, l_m$ and l_{m+1} be the corresponding critical lines. We express a point $p_i(t_i) = (x_i + k_{x_i}t_i, y_i + k_{y_i}t_i, z_i + k_{z_i}t_i)$ on l_i in general form, with $t_i \in \mathbb{R}$, where i equals $0, 1, \dots, \text{or } m + 1$.

In the following, $p(t_i)$ will be denoted by p_i for short, where i equals $0, 1, \dots, \text{or } m + 1$.

Lemma 1. *If $e_1 \perp e_2$, then $\frac{\partial d_e(p_1, p_2)}{\partial t_2}$ can be written as $(t_2 - \alpha)\beta$, where $\beta > 0$, and β is a function of t_1 and t_2 , α is equal to 0 if e_1 and the first end point of e_2 are on the same grid plane, and α is equal to 1 otherwise.*

Proof. Without loss of generality, we can assume that e_2 is parallel to the z -axis. In this case, the parallel projection (denoted by $g'(e_1, e_2)$) of all of g 's cubes, contained between e_1 and e_2 , is illustrated in Figure 2, where AB is the projective image of e_1 , and C is that of one of the end points of e_2 .

Case 1. e_1 and the first end point of e_2 are on the same grid plane. Let the two end points of e_2 be (a, b, c) and $(a, b, c + 1)$. Then the two end points of e_1 are $(a - 1, b + k, c)$ and $(a, b + k, c)$. Then the coordinates of p_1 and p_2 are $(a - 1 + t_1, b + k, c)$ and $(a, b, c + t_2)$ respectively, and $d_e(p_1, p_2) = \sqrt{(t_1 - 1)^2 + k^2 + t_2^2}$. Therefore,

$$\frac{\partial d_e(p_1, p_2)}{\partial t_2} = \frac{t_2}{\sqrt{(t_1 - 1)^2 + k^2 + t_2^2}}$$

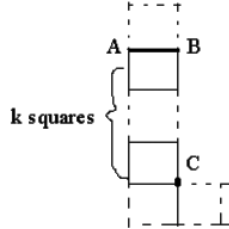


Fig. 2. Illustration for the proof of Lemma 1.

Let $\alpha = 0$ and

$$\beta = \frac{1}{\sqrt{(t_1 - 1)^2 + k^2 + t_2^2}}$$

This proves the lemma for Case 1.

Case 2. Now assume that e_1 and the first end point of e_2 are on different grid planes (i.e., e_1 and the second end point of e_2 are on the same grid plane). Let the two end points of e_2 be (a, b, c) and $(a, b, c + 1)$. Then the two end points of e_1 are $(a - 1, b + k, c + 1)$ and $(a, b + k, c + 1)$. Then the coordinates of p_1 and p_2 are $(a - 1 + t_1, b + k, c + 1)$ and $(a, b, c + t_2)$, respectively, and $d_e(p_1, p_2) = \sqrt{(t_1 - 1)^2 + k^2 + (t_2 - 1)^2}$. Therefore,

$$\frac{\partial d_e(p_1, p_2)}{\partial t_2} = \frac{t_2 - 1}{\sqrt{(t_1 - 1)^2 + k^2 + (t_2 - 1)^2}}$$

Let $\alpha = 1$ and

$$\beta = \frac{1}{\sqrt{(t_1 - 1)^2 + k^2 + (t_2 - 1)^2}}$$

This proves the lemma for Case 2. □

Lemma 2. *If $e_1 \parallel e_2$, then*

$$\frac{\partial d_e(p_1, p_2)}{\partial t_2} = (t_2 - t_1)\beta$$

for some $\beta > 0$, where β is a function of t_1 and t_2 .

Proof. Without loss of generality, we can assume that e_2 is parallel to the z -axis. In this case, the parallel projection (denoted by $g'(e_1, e_2)$) of all of g 's cubes contained between e_1 and e_2 is illustrated in Figure 3, where A is the projective image of one of the end points of e_1 , and B is that of one of the end points of e_2 .

Case 1. Edges e_1 and e_2 are on the same grid plane. Let the two end points of e_2 be (a, b, c) and $(a, b, c + 1)$. Then the two end points of e_1 are $(a, b + k, c)$

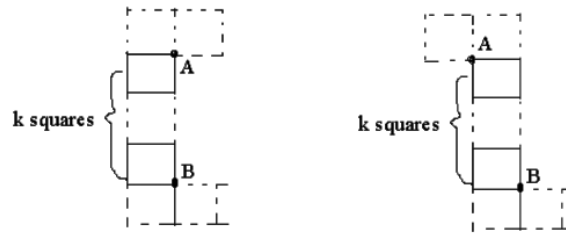


Fig. 3. Illustration for the proof of Lemma 2. Left: Case 1. Right: Case 2.

and $(a, b + k, c + 1)$. Then the coordinates of p_1 and p_2 are $(a, b + k, c + t_1)$ and $(a, b, c + t_2)$, respectively, and $d_e(p_1, p_2) = \sqrt{(t_2 - t_1)^2 + k^2}$. Therefore,

$$\frac{\partial d_e(p_1, p_2)}{\partial t_2} = \frac{t_2 - t_1}{\sqrt{(t_2 - t_1)^2 + k^2}}$$

Let

$$\beta = \frac{1}{\sqrt{(t_2 - t_1)^2 + k^2}}$$

This proves the lemma for Case 1.

Case 2. Now assume that edges e_1 and e_2 are on different grid planes. Let the two end points of e_2 be (a, b, c) and $(a, b, c + 1)$. Then the two end points of e_1 are $(a - 1, b + k, c)$ and $(a - 1, b + k, c + 1)$. Then the coordinates of p_1 and p_2 are $(a - 1, b + k, c + t_1)$ and $(a, b, c + t_2)$ respectively, and $d_e(p_1, p_2) = \sqrt{(t_2 - t_1)^2 + k^2 + 1}$. Therefore,

$$\frac{\partial d_e(p_1, p_2)}{\partial t_2} = \frac{t_2 - t_1}{\sqrt{(t_2 - t_1)^2 + k^2 + 1}}$$

Let

$$\beta = \frac{1}{\sqrt{(t_2 - t_1)^2 + k^2 + 1}}$$

This proves the lemma for Case 2. □

This Lemma will be used later for the proof of Lemma 6. – Let $d_i = d_e(p_{i-1}, p_i) + d_e(p_i, p_{i+1})$, for $i = 1, 2, \dots, m$.

Theorem 2. *If $e_i \perp e_j$, where $i, j = 1, 2, 3$ and $i \neq j$, then e_1, e_2 and e_3 form an endangle iff the equation*

$$\frac{\partial (d_e(p_1, p_2) + d_e(p_2, p_3))}{\partial t_2} = 0$$

has a unique root 0 or 1.

Proof. Without loss of generality, we can assume that e_2 is parallel to the z -axis.

(A) If e_1, e_2 and e_3 form an end angle, then by Definition 4, the z -coordinates of two end points of e_1 and e_3 are equal.

Case A1. Edges e_1, e_3 and the first end point of e_2 are on the same grid plane. By Lemma 1,

$$\frac{\partial (d_e(p_1, p_2))}{\partial t_2} = (t_2 - \alpha_1)\beta_1$$

where $\alpha_1 = 0$ and $\beta_1 > 0$, and

$$\frac{\partial (d_e(p_2, p_3))}{\partial t_2} = (t_2 - \alpha_2)\beta_2$$

where $\alpha_2 = 0$ and $\beta_2 > 0$. So we have

$$\frac{\partial(d_e(p_1, p_2) + d_e(p_2, p_3))}{\partial t_2} = t_2(\beta_1 + \beta_2)$$

Therefore, the equation of the theorem has the unique root $t_2 = 0$.

Case A2. Edges e_1 , e_3 and the second end point of e_2 are on the same grid plane. By Lemma 1,

$$\frac{\partial(d_e(p_1, p_2))}{\partial t_2} = (t_2 - \alpha_1)\beta_1$$

where $\alpha_1 = 1$ and $\beta_1 > 0$, and

$$\frac{\partial(d_e(p_2, p_3))}{\partial t_2} = (t_2 - \alpha_2)\beta_2$$

where $\alpha_2 = 1$ and $\beta_2 > 0$. So we have

$$\frac{\partial(d_e(p_1, p_2) + d_e(p_2, p_3))}{\partial t_2} = (t_2 - 1)(\beta_1 + \beta_2)$$

Therefore, the equation of the theorem has the unique root $t_2 = 1$.

(B) Conversely, if the equation of the theorem has a unique root 0 or 1, then e_1 , e_2 and e_3 form an end angle. Otherwise, e_1 , e_2 and e_3 form an inner angle. By Definition 4, the z -coordinates of two end points of e_1 are not equal to z -coordinates of two end points of e_3 (Note: Without loss of generality, we can assume that $e_2 \parallel z$ -axis.). So e_1 and e_3 are not on the same grid plane.

Case B1. Edge e_1 and the first end point of e_2 are on the same grid plane, while e_3 and the second end point of e_2 are on the same grid plane. By Lemma 1,

$$\frac{\partial(d_e(p_1, p_2))}{\partial t_2} = (t_2 - \alpha_1)\beta_1$$

where $\alpha_1 = 0$ and $\beta_1 > 0$, while

$$\frac{\partial(d_e(p_2, p_3))}{\partial t_2} = (t_2 - \alpha_2)\beta_2$$

where $\alpha_2 = 1$ and $\beta_2 > 0$. So we have

$$\frac{\partial(d_e(p_1, p_2) + d_e(p_2, p_3))}{\partial t_2} = t_2\beta_1 + (t_2 - 1)\beta_2$$

Therefore $t_2 = 0$ or 1 is not a root of the equation of the theorem. This is a contradiction.

Case B2. Edge e_1 and the second end point of e_2 are on the same grid plane, while e_3 and the first end point of e_2 are on the same grid plane. By Lemma 1,

$$\frac{\partial(d_e(p_1, p_2))}{\partial t_2} = (t_2 - \alpha_1)\beta_1$$

where $\alpha_1 = 1$ and $\beta_1 > 0$, while

$$\frac{\partial(d_e(p_2, p_3))}{\partial t_2} = (t_2 - \alpha_2)\beta_2$$

where $\alpha_2 = 0$ and $\beta_2 > 0$. So we have

$$\frac{\partial(d_e(p_1, p_2) + d_e(p_2, p_3))}{\partial t_2} = (t_2 - 1)\beta_1 + t_2\beta_2$$

Therefore, $t_2 = 0$ or 1 is not a root of the equation of the theorem. This is a contradiction as well. \square

2.2 Theorem on Inner Angles

Theorem 3. *If $e_i \perp e_j$, where $i, j = 1, 2, 3$ and $i \neq j$, then e_1, e_2 and e_3 form an inner angle iff the equation*

$$\frac{\partial(d_e(p_1, p_2) + d_e(p_2, p_3))}{\partial t_2} = 0$$

has a root t_{2_0} such that $0 < t_{2_0} < 1$.

Proof. If edges e_1, e_2 and e_3 form an inner angle, then by Definition 4, e_1, e_2 and e_3 do not form an end angle. By Theorem 2, 0 or 1 is not a root of the equation of the theorem. By Lemma 1,

$$\frac{\partial(d_e(p_1, p_2) + d_e(p_2, p_3))}{\partial t_2} = (t_2 - \alpha_1)\beta_1 + (t_2 - \alpha_2)\beta_2$$

where α_1, α_2 are 0 or 1 , $\beta_1 > 0$ is a function of t_1 and t_2 , and $\beta_2 > 0$ is a function of t_2 and t_3 . So $\alpha_1 \neq \alpha_2$ (i.e., $\alpha_1 = 0$ and $\alpha_2 = 1$ or $\alpha_1 = 1$ and $\alpha_2 = 0$). Therefore, the equation of the theorem has a root t_{2_0} such that $0 < t_{2_0} < 1$.

Conversely, if the equation of the theorem has a root t_{2_0} such that $0 < t_{2_0} < 1$, then by Theorem 2, critical edges e_1, e_2 and e_3 do not form an end angle. By Definition 4, e_1, e_2 and e_3 do form an inner angle. \square

2.3 Grid Plane Characterization Theorem

Assume that $e_0 \perp e_1, e_2 \perp e_3$, and $e_1 \parallel e_2$. Assume that $p(t_{i_0})$ is a vertex of the MLP of g , where $i = 1$ or $i = 2$. Then we have the following:

Lemma 3. *If e_0, e_3 and the first end point of e_1 are on the same grid plane, and t_{i_0} is a root of*

$$\frac{\partial d_i}{\partial t_i} = 0$$

then $t_{i_0} = 0$, where $i = 1$ or $i = 2$.

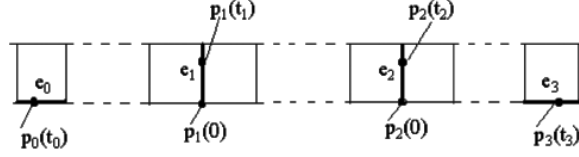


Fig. 4. Illustration of the proof of Lemma 3.

Proof. From $p_0(t_0)p_1(0) \perp e_1$ it follows that

$$d_e(p_0(t_0)p_1(0)) = \min\{d_e(p_0(t_0), p_1(t_1)) : t_1 \in [0, 1]\}$$

(see Figure 4). Analogously, we have

$$d_e(p_2(0)p_3(t_3)) = \min\{d_e(p_2(t_2), p_3(t_3)) : t_2 \in [0, 1]\}$$

and

$$d_e(p_1(0)p_2(0)) = \min\{d_e(p_1(t_1), p_2(t_2)) : t_1, t_2 \in [0, 1]\}$$

Therefore we have

$$\begin{aligned} & \min\{d_e(p_0(t_0), p_1(t_1)) + d_e(p_1(t_1), p_2(t_2)) + d_e(p_2(t_2), p_3(t_3)) : t_1, t_2 \in [0, 1]\} \\ & \geq d_e(p_0(t_0), p_1(0)) + d_e(p_1(0), p_2(0)) + d_e(p_2(0), p_3(t_3)) \end{aligned}$$

This proves the lemma. \square

Assume that we have $e_0 \perp e_1$, $e_m \perp e_{m+1}$, and $e_i \parallel e_{i+1}$, (i.e., the set $\{e_1, e_2, \dots, e_m\}$ is a maximal run of parallel critical edges of g , and e_0 or e_{m+1} are the adjacent critical edges of this set). Furthermore, let $p(t_{i_0})$ be a vertex of the MLP of g , where $i = 1, 2, \dots, m-1$. Analogously to the previous lemma, we also have the following two lemmas:

Lemma 4. *If e_0 , e_{m+1} and the first point of e_1 are on the same grid plane, and t_{i_0} is a root of*

$$\frac{\partial d_i}{\partial t_i} = 0$$

then $t_{i_0} = 0$, where $i = 1, 2, \dots, m$.

Lemma 5. *If e_0 , e_{m+1} and the second end point of e_1 are on the same grid plane, and t_{i_0} is a root of*

$$\frac{\partial d_i}{\partial t_i} = 0$$

then $t_{i_0} = 1$, where $i = 1, 2, \dots, m$.

Now we study the case that critical edges are on different grid planes. (Note that even two parallel edges can be on different grid planes.)

Lemma 6. If e_0 and e_{m+1} are on different grid planes, and t_{i_0} is a root of

$$\frac{\partial d_i}{\partial t_i} = 0$$

where $i = 1, 2, \dots, m$, then $0 < t_1 < t_2 < \dots < t_m < 1$.

Proof. Assume that e_0 and the first end point of e_1 are on the same grid plane, and e_{m+1} and the second end point of e_1 are on the same grid plane. Then (by Lemmas 1 and 2), the derivatives $\frac{\partial d_i}{\partial t_i}$, where $i = 1, 2, \dots, m$, have the following forms:

$$\begin{aligned} \frac{\partial d_1}{\partial t_1} &= t_1 b_{1_1} + (t_1 - t_2) b_{1_2} \\ \frac{\partial d_2}{\partial t_2} &= (t_2 - t_1) b_{2_1} + (t_2 - t_3) b_{2_2} \\ \frac{\partial d_3}{\partial t_3} &= (t_3 - t_2) b_{3_1} + (t_3 - t_4) b_{3_2} \\ &\dots \\ \frac{\partial d_{m-1}}{\partial t_{m-1}} &= (t_{m-1} - t_{m-2}) b_{m-1_1} + (t_{m-1} - t_m) b_{m-1_2}, \text{ or} \\ \frac{\partial d_m}{\partial t_m} &= (t_m - t_{m-1}) b_{m_1} + (t_m - 1) b_{m_2} \end{aligned} \quad (1)$$

where $b_{i_1} > 0$, b_{i_1} is a function of t_i and t_{i-1} , $b_{i_2} > 0$, and b_{i_2} is a function of t_i and t_{i+1} , for $i = 1, 2, \dots, m$.

If $t_{1_0} < 0$, then (by $\frac{\partial d_1}{\partial t_1} = 0$) we have that $t_{1_0} b_{1_1} + (t_{1_0} - t_{2_0}) b_{1_2} = 0$. Since $b_{1_1} > 0$ and $b_{1_2} > 0$, we also have $t_{1_0} - t_{2_0} > 0$ (i.e., $t_{1_0} > t_{2_0}$).

Analogously, because of $\frac{\partial d_2}{\partial t_2} = 0$ we have $(t_{2_0} - t_{1_0}) b_{2_1} + (t_{2_0} - t_{3_0}) b_{2_2} = 0$. This means that we also have $t_{2_0} > t_{3_0}$.

Analogously we can also verify that $t_{3_0} > t_{4_0}, \dots$, and $t_{m-1_0} > t_{m_0}$. Therefore, by Equation (1) we have $t_{m_0} - 1 > 0$. Altogether we have $0 > t_{1_0} > t_{2_0} > t_{3_0} > \dots > t_{m_0} > 1$. This is an obvious contradiction.

If $t_{1_0} = 0$, then (by $\frac{\partial d_1}{\partial t_1} = 0$) we have that $t_{2_0} = 0$. Analogously, $\frac{\partial d_2}{\partial t_2} = 0$ implies $t_{3_0} = 0$, and we also have $t_{4_0} = 0, \dots, t_{m_0} = 0$ due to the same argument. But, by Equation (1) we have

$$\frac{\partial d_m}{\partial t_m} = (t_m - 1) b_{m_2} = -b_{m_2} < 0$$

This contradicts $\frac{\partial d_m}{\partial t_m} = 0$.

If $t_{1_0} \geq 1$, then (by $\frac{\partial d_1}{\partial t_1} = 0$) we have $t_{1_0} b_{1_1} + (t_{1_0} - t_{2_0}) b_{1_2} = 0$. Due to $b_{1_1} > 0$ and $b_{1_2} > 0$ we have $t_{1_0} - t_{2_0} < 0$ (i.e., $t_{1_0} < t_{2_0}$). Analogously, by $\frac{\partial d_2}{\partial t_2} = 0$ it follows that $(t_{2_0} - t_{1_0}) b_{2_1} + (t_{2_0} - t_{3_0}) b_{2_2} = 0$. Then we have $t_{2_0} < t_{3_0}$, and we also have $t_{3_0} < t_{4_0}, \dots, t_{m-1_0} < t_{m_0}$. Therefore, by Equation (1) we have $t_{m_0} - 1 < 0$. Altogether we have $1 \leq t_{1_0} < t_{2_0} < t_{3_0} < \dots < t_{m_0} < 1$, which is again an obvious contradiction. \square

Let t_{i_0} be a root of $\frac{\partial d_i}{\partial t_i} = 0$, where $i = 1, 2, \dots, m$. We apply Lemmas 4, 5 and 6 and obtain

Theorem 4. *Edges e_0 and e_{m+1} are on different grid planes iff $0 < t_{1_0} < t_{2_0} < \dots < t_{m_0} < 1$.*

2.4 Basics for a Necessary Correction of Option 3

The following two Lemmas will be used in Section 5 when revising Option 3 of the original rubberband algorithm. Let p_1, p_2 be points on a critical edge e_i of curve g , and p a point on a critical edge e_j of g .

Lemma 7. *If the line segments pp_1, pp_2 are contained and complete in tube \mathbf{g} , then the triangular region $\Delta(p_1, p_2, p)$ is also contained and complete in \mathbf{g} .*

Proof. Without loss generality, we can assume that $i < j$. Let $a(e_i, e_j)$ be the arc from the first cube which contains the critical edge e_i to the last cube which contains the critical edge e_j . (Note that a set of consecutive critical edges will uniquely define a cube-curve.) If line segments pp_1, pp_2 are contained and complete in \mathbf{g} , then the xy - (yz - and xz -) projection of $\Delta(p_1, p_2, p)$ is contained and complete in the xy - (yz - and xz -) projection of $a(e_i, e_j)$. Therefore, the triangular region $\Delta(p_1, p_2, p)$ is contained and complete in the tube of $a(e_i, e_j)$. \square

Lemma 8. *Let $d_2(t_1, t_2, t_3) = d_e(p_1, p_2) + d_e(p_2, p_3)$. It follows that $d_2(t_1, t_2, t_3)$ is increasing with respect to t_2 .*

Proof. Let the coordinates of p_i be $(x_i + k_{x_i}t_i, y_i + k_{y_i}t_i, z_i + k_{z_i}t_i)$, where i equals 1 or 3. Since $p_i \in e_i \subset l_i$, and e_i is a critical edge which is an edge of an orthogonal grid, only one of the values k_{x_i}, k_{y_i} and k_{z_i} can be 1 and the other two must be zero. We consider one of these cases where the coordinates of p_1 are $(x_1 + t_1, y_1, z_1)$, the coordinates of p_2 are $(x_2, y_2 + t_2, z_2)$, and the coordinates of p_3 are $(x_3, y_3, z_3 + t_3)$. Then

$$\begin{aligned} d_2 &= d_e(p_1, p_2) + d_e(p_2, p_3) \\ &= \sqrt{(t_2 - (y_1 - y_2))^2 + (x_1 + t_1 - x_2)^2 + (z_1 - z_2)^2} \\ &\quad + \sqrt{(t_2 - (y_3 - y_2))^2 + (x_3 - x_2)^2 + (z_3 + t_3 - z_2)^2} \end{aligned}$$

This can be rewritten as $d_2 = \sqrt{(t_2 - a_1)^2 + b_1^2} + \sqrt{(t_2 - a_2)^2 + b_2^2}$, where b_1 and b_2 are functions of t_1 and t_3 . Then we have

$$\frac{\partial d_2}{\partial t_2} = \frac{t_2 - a_1}{\sqrt{(t_2 - a_1)^2 + b_1^2}} + \frac{t_2 - a_2}{\sqrt{(t_2 - a_2)^2 + b_2^2}} \quad (2)$$

and

$$\begin{aligned} \frac{\partial^2 d_2}{\partial t_2^2} &= \frac{1}{\sqrt{(t_2 - a_1)^2 + b_1^2}} - \frac{(t_2 - a_1)^2}{[(t_2 - a_1)^2 + b_1^2]^{3/2}} \\ &\quad + \frac{1}{\sqrt{(t_2 - a_2)^2 + b_2^2}} - \frac{(t_2 - a_2)^2}{[(t_2 - a_2)^2 + b_2^2]^{3/2}} \end{aligned}$$

This simplifies to

$$\frac{\partial^2 d_2}{\partial t_2^2} = \frac{b_1^2}{[(t_2 - a_1)^2 + b_1^2]^{3/2}} + \frac{b_2^2}{[(t_2 - a_2)^2 + b_2^2]^{3/2}} > 0 \quad (3)$$

This implies that $d_2(t_1, t_2, t_3)$ is increasing with respect to t_2 . All other cases follow analogously. \square

3 Theorem about Linear Time Complexity

A *polygonal path* is a continuous arc composed of one or more line segments; it is *simple* iff only two consecutive line segments of it intersect, and they do so only intersect at one of their endpoints.

Let $Q_i(x_i, y_i, 0)$ be the projection of $P_i(x_i, y_i, z_i)$ onto the xy -plane, where $i = 1, 2$ (see Figure 5).

Lemma 9. *If Q_2 is on the left of OQ_1 then P_2 is on the left of OP_1 .*

Proof. Since $\triangle OP_1P_2$ can be obtained by continuously moving Q_i to P_i , where $i = 1, 2$. \square

Lemma 10. *Option 2 of the rubberband algorithm (see Appendix 1) can be computed in $\mathcal{O}(m)$ time, where m is the number of critical edges intersected by the polygonal path between p_{i-1} and p_{i+1} .*

Proof. We start with vertices of the initial polygon at center points of each critical edge of the given cube-curve.

It follows that the vertices of a resulting polygon, using only Option 1 of the rubberband algorithm, are still at the center points of critical edges.

Option 2 of the algorithm can now be implemented as follows: Let \mathcal{A} be the cube-arc starting at the first cube which contains critical edge e_{i-1} , to the last cube which contains critical edge e_{i+1} . Proceed as follows:

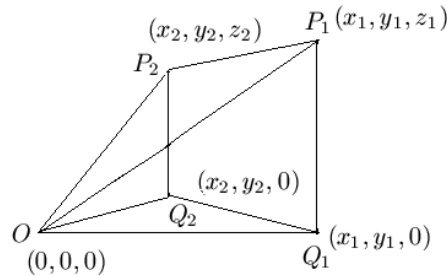


Fig. 5. Illustration for Lemma 9.

1. Compute all the intersection points, denoted by S_I , of the closed triangular region $\Delta(p_{i-1}, p_i, p_{i+1})$ with consecutive critical edges from e_{i-1} to e_{i+1} (note: they are between both endpoints of a critical edge). This can be computed in $\mathcal{O}(m_1)$ time, where $m_1 = |S_I| \leq$ is the number of critical edges in \mathcal{A} .

2. Let S_P be the set of three planes: xy -plane, yz -plane, and zx -plane. Select a plane $\alpha \in S_P$, such that α is not perpendicular to $\Delta(p_{i-1}, p_i, p_{i+1})$. This can be computed in $\mathcal{O}(1)$ time,

3. Project S_I onto α . Let the resulting set be S'_I .

4. Apply the Melkman algorithm [9] (which is linear, see [12]) to find the convex arc, denoted by \mathcal{A}' in α .

5. By Lemma 9 (the projection of the convex hull of S_I onto α is the convex hull of S'_I); compute a convex arc, denoted by \mathcal{A}'' , in $\Delta(p_{i-1}, p_i, p_{i+1})$ such that the projection of \mathcal{A}'' onto α is \mathcal{A}' .

6. If there exists a vertex v of \mathcal{A}'' such that v is not inside of the tube g , then remove v from S_I . Go to Step 3. Otherwise, replace \mathcal{A} by \mathcal{A}'' and Stop.

Each of the Steps 3 to 6 can be computed in $\mathcal{O}(m_2)$ time, where $m_2 = |S'_I| = |S_I| \leq$ the number of critical edges in \mathcal{A} .

Altogether, it follows that the convex arc can be computed in $\mathcal{O}(m)$ time, where m is the number of critical edges intersecting the arc between p_{i-1} and p_{i+1} . \square

Lemma 11. *Point $p_1 \in e_1$, defined by $d_e(p_1, p_0) + d_e(p_1, p_2) = \min\{p_1 | d_e(p_1, p_0) + d_e(p_1, p_2), p_1 \in e_2\}$, can be computed in $\mathcal{O}(1)$ time.*

Proof. Let the two endpoints of e_1 be $a_1(a_{11}, a_{12}, a_{13})$ and $b_1(b_{11}, b_{12}, b_{13})$. Let the coordinates of p_0 be (p_{01}, p_{02}, p_{03}) . p_1 can be written as $(a_{11} + (b_{11} - a_{11})t, a_{12} + (b_{12} - a_{12})t, a_{13} + (b_{13} - a_{13})t)$. The formula

$$d_e(p_1, p_0) = \sqrt{\sum_{i=1}^3 ((a_{1i} - p_{0i}) + (b_{1i} - a_{1i})t)^2}$$

can be simplified: The straight line $a_1 b_1$ is isothetic (i.e., parallel to one of the three coordinate axes). It follows that only one element of the set $\{b_{1i} - a_{1i} : i = 1, 2, 3\}$ is equal to 1, and the other two are equal to 0. Without loss of generality we can assume that

$$d_e(p_1, p_0) = \sqrt{(t + A_1)^2 + B_1}$$

where A_1 and B_1 are functions of a_{1i}, b_{1i} and p_{0i} , for $i = 0, 1, 2$. - Analogously,

$$d_e(p_1, p_2) = \sqrt{(t + A_2)^2 + B_2}$$

where A_2 and B_2 are functions of a_{1i}, b_{1i} and p_{2i} , for $i = 0, 1, 2$. In order to find a point $p_1 \in e_1$ such that $d_e(p_1, p_0) + d_e(p_1, p_2) = \min\{p_1 | d_e(p_1, p_0) + d_e(p_1, p_2), p_1 \in e_1\}$, we can solve the equation

$$\frac{\partial(d_e(p_1, p_0) + d_e(p_1, p_2))}{\partial t} = 0$$

The unique solution is $t = -(A_1 B_2 + A_2 B_1) / (B_2 + B_1)$. \square

Theorem 5. *The rubberband algorithm has linear time complexity $\mathcal{O}(m)$, where m is the number of critical edges of the given simple cube curve.*

Proof. Lemma 10 implies that all operations in Option 2 of the rubberband algorithm can be computed in $\mathcal{O}(m)$ time. Lemma 11 implies that all operations in Option 3 of the algorithm can be computed in $\mathcal{O}(m)$ time. This proves the theorem. \square

4 Example of a “Difficult” Simple Cube Curve

We provide an example to show that there are simple cube-curves such that none of the vertices of its MLP is a grid vertex. See Figure 6 and Table 1 for an example of such a cube-curve, which lists the coordinates of the critical edges e_0, e_1, \dots, e_{19} of g . Let $v(t_0), v(t_1), \dots, v(t_{19})$ be the vertex of the MLP of g such that $v(t_i)$ is on e_i and t_i is in $[0, 1]$, where $i = 0, 1, 2, \dots, 19$.

See Appendix 2 for a complete list of all $\frac{\partial d_i}{\partial t_i}$ ($i = 0, 1, \dots, 19$) for this cube-curve g . It follows that there is no end angle in g , but we have six inner angles:

$$\angle(e_2, e_3, e_4), \angle(e_3, e_4, e_5), \angle(e_6, e_7, e_8), \angle(e_9, e_{10}, e_{11}), \angle(e_{10}, e_{11}, e_{12}),$$

$$\text{and } \angle(e_{13}, e_{14}, e_{15}).$$

By Theorem 3 we have that $t_3, t_4, t_7, t_{10}, t_{11}$ and t_{14} are all in the open interval $(0, 1)$. — Figure 6 shows that $e_1 \parallel e_2$, and e_0 and e_3 are on different grid planes. By Theorem 4 it follows that t_1 and t_2 are in $(0, 1)$, too. Analogously we have that t_5 and t_6 are in $(0, 1)$, t_8 and t_9 are in $(0, 1)$, t_{12} and t_{13} are in $(0, 1)$, t_{15}, t_{16} and t_{17} are in $(0, 1)$, and t_{18}, t_{19} and t_0 are in $(0, 1)$. Therefore, each t_i is in the open interval $(0, 1)$, where $i = 0, 1, \dots, 19$, which proves that g is a simple cube-curve such that none of the vertices of its MLP is a grid vertex.

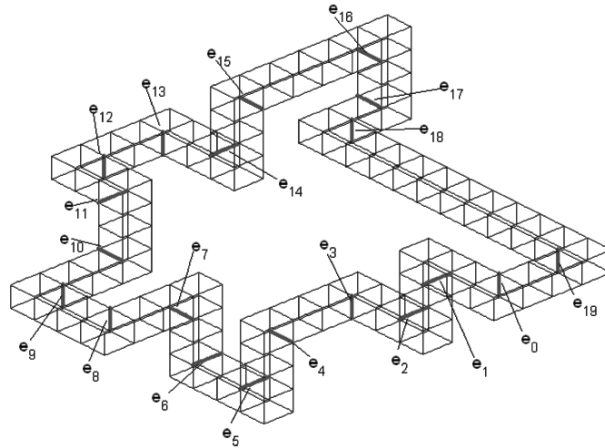


Fig. 6. A simple cube-curve such that none of the vertices of its MLP is a grid vertex.

| Critical edge | x_{i1} | y_{i1} | z_{i1} | x_{i2} | y_{i2} | z_{i2} |
|---------------|----------|----------|----------|----------|----------|----------|
| e_0 | -1 | 4 | 7 | -1 | 4 | 8 |
| e_1 | 1 | 4 | 7 | 1 | 5 | 7 |
| e_2 | 2 | 4 | 5 | 2 | 5 | 5 |
| e_3 | 4 | 5 | 4 | 4 | 5 | 5 |
| e_4 | 4 | 7 | 4 | 5 | 7 | 4 |
| e_5 | 5 | 7 | 2 | 5 | 8 | 2 |
| e_6 | 7 | 7 | 2 | 7 | 8 | 2 |
| e_7 | 7 | 8 | 4 | 8 | 8 | 4 |
| e_8 | 8 | 10 | 4 | 8 | 10 | 5 |
| e_9 | 10 | 10 | 4 | 10 | 10 | 5 |
| e_{10} | 10 | 8 | 5 | 11 | 8 | 5 |
| e_{11} | 11 | 7 | 7 | 11 | 8 | 7 |
| e_{12} | 12 | 7 | 7 | 12 | 7 | 8 |
| e_{13} | 12 | 5 | 7 | 12 | 5 | 8 |
| e_{14} | 10 | 4 | 8 | 10 | 5 | 8 |
| e_{15} | 9 | 4 | 10 | 10 | 4 | 10 |
| e_{16} | 9 | 0 | 10 | 10 | 0 | 10 |
| e_{17} | 9 | 0 | 8 | 10 | 0 | 8 |
| e_{18} | 9 | 1 | 7 | 9 | 1 | 8 |
| e_{19} | -1 | 2 | 7 | -1 | 2 | 8 |

Table 1. Coordinates of endpoints of critical edges of the curve of Figure 6.

5 Corrected Rubberband Algorithm

The rubberband algorithm was published in [1] and [7], and the iteration steps of this (original) algorithm are given in Appendix 1.

Figure 7 shows a non-first-class simple cube-curve (see Table 2 in Appendix 2 for the data of this curve). The figure also shows the resulting polygons of three options of the original rubberband algorithm.

We start with the polygonal curve L_1 . After applying Option 1 we obtain the curve L_2 . Then we apply Option 2 and obtain the curve L_3 . Finally we apply Option 3 as given in the original rubberband algorithm and we obtain curve L_4 as final result.

For the resulting polygon L_4 note that edge $p(t_{9_0})p(t_{13_0})$ is not contained in the tube \mathbf{g} . This means that the final polygon is not contained in the tube \mathbf{g} ! This is because Option 3 of the original algorithm did not check whether $p_{i-1}p_{new}$ and $p_{new}p_{i+1}$ are both contained in the tube \mathbf{g} . A minor but essential correction is required to fix this problem.

The figure also shows the corrected polygon L_5 . Note that edge $p(\bar{t}_{9_0})p(\bar{t}_{13_0})$ is now contained in the tube \mathbf{g} .

Figure 8 also shows that there are cases where non of the two endpoints of an edge of the polygonal curve (resulting from Option 2) is allowed any move across a critical edge (This allows a further modification of the original Option

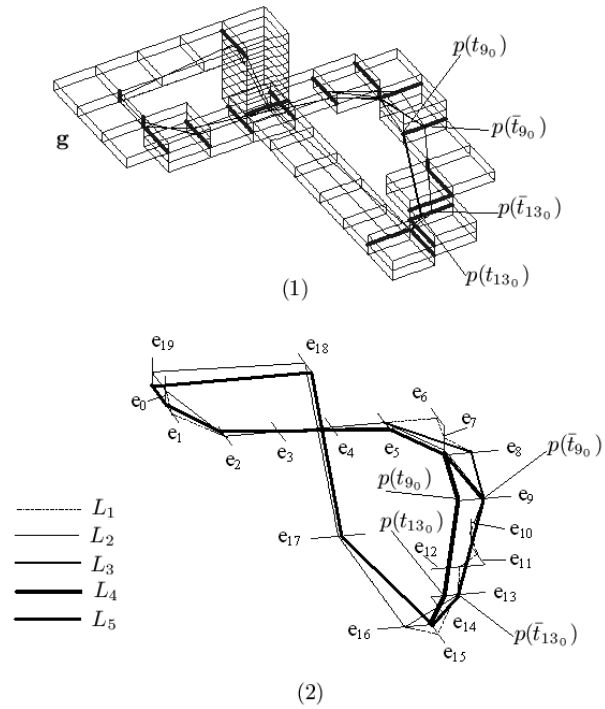


Fig. 7. An Example of a non-first-class simple cube-curve. The figure shows resulting polygons when applying options of the original or of the corrected rubberband algorithm, respectively. (1) shows that edge $p(t_{90})p(t_{130})$ is not contained in the tube g while $p(\bar{t}_{90})p(\bar{t}_{130})$ is contained in it. (2) shows the polygons of (1) with all the cubes removed.

3, denoted by (O_3) .): We consider c_1, c_2 which are two cubes, and two critical edges e_1, e_2 . Line p_1p_2 is contained and complete in the arc from the cube which contains e_1 to the cube which contains e_2 . p_1p_2 intersects with c_1 and c_2 only at

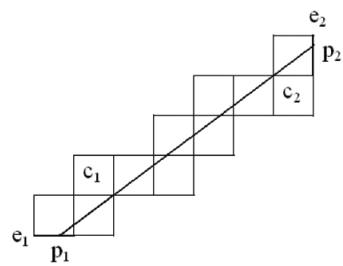


Fig. 8. An example where any move of one of the two end points of a line segment along critical edges is impossible.

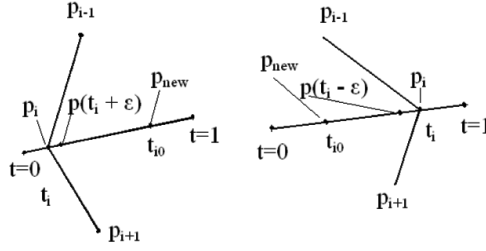


Fig. 9. Illustration of Option 3. Left: Case 1. Right: Case 2.

a single point each. If p_1 moves to the left along e_1 , then p_1p_2 will not intersect with c_2 anymore. If p_1 moves to the right along e_1 , then p_1p_2 will not intersect with c_1 anymore. If p_2 moves up along e_2 , then p_1p_2 will not intersect with c_2 anymore. If p_2 moves down along e_2 , then p_1p_2 will not intersect with c_1 anymore.

The following (revised) Option 3 ensures that the final polygon is always contained and complete in the tube \mathbf{g} . We use Figure 9 for illustration of the revised Option 3:

Let $p_i = p_i(t_i)$ and $p_{new} = p_i(t_{i0})$. By (O_3) , $t_i, t_{i0} \in [0, 1]$. Let ε be a sufficiently small positive real number.

(Case 1) $t_i < t_{i0}$ (see Figure 9 on the left):

(Case 1.1) both $p_{i-1}p(t_i + \varepsilon)$ and $p_{i+1}p(t_i + \varepsilon)$ are inside the arc from p_{i-1} to p_{i+1} : If both $p_{i-1}p_{new}$ and $p_{i+1}p_{new}$ are inside the arc from e_{i-1} to e_{i+1} , then $\bar{p}_{new} = p_{new}$. Otherwise, by Lemmas 7 and 8, use binary search to find a value $\bar{t}_{i0} \in (t_i, t_{i0})$, and then let $\bar{p}_{new} = p(\bar{t}_{i0})$.

(Case 1.2) either $p_{i-1}p(t_i + \varepsilon)$ or $p_{i+1}p(t_i + \varepsilon)$ are outside the arc from e_{i-1} to e_{i+1} : Then let $\bar{p}_{new} = p_i(t_i) = p_i$.

(Case 2) $t_{i0} < t_i$ (see Figure 9 on the right):

(Case 2.1) both $p_{i-1}p(t_i - \varepsilon)$ and $p_{i+1}p(t_i - \varepsilon)$ are inside the arc from p_{i-1} to p_{i+1} : If both $p_{i-1}p_{new}$ and $p_{i+1}p_{new}$ are inside the arc from e_{i-1} to e_{i+1} , then $\bar{p}_{new} = p_{new}$. Otherwise, (again by Lemmas 7 and 8) use binary search to find a value $\bar{t}_{i0} \in (t_{i0}, t_i)$, and then let $\bar{p}_{new} = p(\bar{t}_{i0})$.

(Case 2.2) either $p_{i-1}p(t_i - \varepsilon)$ or $p_{i+1}p(t_i - \varepsilon)$ are outside the arc from e_{i-1} to e_{i+1} : Then let $\bar{p}_{new} = p_i(t_i) = p_i$.

This revised Option 3 contains the test of inclusion (which was missing in the original algorithm), and it details the steps for minimizing the length of the calculated polygonal curve, providing a more specific description of Option 3 compared to the original presentation of the rubberband algorithm.

6 Conclusions

We constructed a non-trivial simple cube-curve such that none of the vertices of its MLP is a grid vertex. Indeed, Theorems 2 and 4, and Lemmas 5 and 6 allow

the conclusion that given a simple first-class cube-curve g , none of the vertices of its MLP is at a grid point position iff g has not any end angle, and for every maximal run of parallel edges of g , its two adjacent critical edges are not on the same grid plane.

It follows that the (provable correct) MLP algorithm proposed in [8] cannot be applied to this curve, because this algorithm requires at least one end angle for decomposing a given cube-curve into arcs. Of course, the rubberband algorithm is applicable, and will produce a result (i.e., a polygonal curve). However, in this case we are still unable to show whether this result is (always) the MLP of the given cube-curve or not. So far, in a large number of experiments (using randomly generated simple cube-curves as input), no incorrect result has been detected (after fixing Option 3 as described above).

Acknowledgements. Reviewers' comments have been very helpful for revising an earlier version of this paper, and they are very much appreciated.

References

1. T. Bülow and R. Klette. Digital curves in 3D space and a linear-time length estimation algorithm. *IEEE Trans. Pattern Analysis Machine Intelligence*, 24:962–970, 2002.
2. J. Canny and J. H. Reif. New lower bound techniques for robot motion planning problems. In Proc. *Foundations Computer Science*, pages 49–60, IEEE Press, 1987.
3. J. Choi, J. Sellen, and C.-K. Yap. Approximate Euclidean shortest path in 3-space. In Proc. *Computational Geometry*, pages 41–48, ACM Press, 1994.
4. E. Ficarra, L. Benini, E. Macii, and G. Zuccheri. Automated DNA fragments recognition and sizing through AFM image processing. *IEEE Trans. Inf. Technol. Biomed.*, 9:508–517, 2005.
5. A. Jonas and N. Kiryati. Length estimation in 3-D using cube quantization, *J. Math. Imaging and Vision*, 8: 215–238, 1998.
6. R. Klette and T. Bülow. Critical edges in simple cube-curves. In Proc. *DGCI*, LNCS 1953, 467-478, 2000.
7. R. Klette and A. Rosenfeld. *Digital Geometry: Geometric Methods for Digital Picture Analysis*. Morgan Kaufmann, San Francisco, 2004.
8. F. Li and R. Klette. Minimum-length polygon of a simple cube-curve in 3D space. In Proc. *Int. Workshop Combinat. Image Analysis*, pages 502–511, LNCS 3322, Springer, Berlin 2004.
9. A. Melkman. On-line construction of the convex hull of a simple polygon. *Information Processing Letters*, 25:11–12, 1987.
10. F. Sloboda, B. Zafko, and R. Klette. On the topology of grid continua. In Proc. *Vision Geometry*, pages 52–63, Vol. 3454, SPIE Press, 1998.
11. F. Sloboda, B. Zafko, and J. Stoer. On approximation of planar one-dimensional grid continua. In *Advances in Digital and Computational Geometry* (R. Klette, A. Rosenfeld, and F. Sloboda, editors), pages 113–160, Springer, Singapore, 1998.
12. D. Sunday. Algorithm 15: convex hull of a 2D simple polygonal path. See [http : //www.softsurfer.com/Archive/algorithm_0203/](http://www.softsurfer.com/Archive/algorithm_0203/) (last visit: November 2005).
13. R. Wolber, F. Stäb, H. Max, A. Wehmeyer, I. Hadshiew, H. Wenck, F. Rippeke, and K. Wittern. Alpha-Glucosylrutin: Ein hochwirksams Flavonoid zum Schutz vor oxidativem Stress. *J. German Society Dermatology*, 2:580–587, 2004.

Appendix 1: Iteration steps of the rubberband algorithm

Let $P_t = (p_0, p_1, \dots, p_m)$ be a polygonal curve contained in a tube \mathbf{g} . A polygonal curve Q is a g -transform of P iff Q may be obtained from P by a finite number of steps, where each step is a replacement of a triple a, b, c of vertices by a polygonal sequence a, b_1, \dots, b_k, c such that the polygonal sequence a, b_1, \dots, b_k, c is contained in the same set of cubes of g as the polygonal sequence a, b, c .

Assume a polygonal curve $P_t = (p_0, p_1, \dots, p_m)$ and three pointers addressing vertices at positions $i-1, i$ and $i+1$ in this curve. There are three different *options* that may occur which define a specific g -transform:

(O_1) Point p_i can be deleted iff $p_{i-1}p_{i+1}$ is a line segment within the tube. Then the subsequence (p_{i-1}, p_i, p_{i+1}) is replaced in the curve by (p_{i-1}, p_{i+1}) . In this case, the algorithm continues with vertices $p_{i-1}, p_{i+1}, p_{i+2}$.

(O_2) The closed triangular region $\Delta(p_{i-1}, p_i, p_{i+1})$ intersects more than just three critical edges of p_{i-1}, p_i and p_{i+1} (i.e., a simple deletion of p_i would not be sufficient anymore). This situation is solved by calculating a convex arc and by replacing point p_i by a sequence of vertices q_1, \dots, q_k on this convex arc between p_{i-1} and p_{i+1} such that the sequence of line segments $p_{i-1}q_1, \dots, q_k p_{i+1}$ lies within the tube. In this case, the algorithm continues with a triple of vertices starting with the calculated new vertex q_k . If (O_1) and (O_2) do not lead to any change, the third option may lead to an improvement (i.e., a shorter polygonal curve which is still contained and complete in the given tube).

(O_3) Point p_i may be moved on its critical edge to obtain an optimum position p_{new} minimizing the total length of both line segments $p_{i-1}p_{new}$ and $p_{new}p_{i+1}$. First, find $p_{opt} \in l_e$ such that $|p_{opt} - p_{i-1}| + |p_{opt} - p_{i+1}| = \min_{p \in l_e} L(p)$ with $L(p) = |p - p_{i-1}| + |p - p_{i+1}|$. Then, if p_{opt} lies on the closed critical edge e , let $p_{new} = p_{opt}$. Otherwise, let p_{new} be that vertex bounding e and lying closest to p_{opt} .

Note that Option 3 of this original rubberband algorithm is not asking for testing inclusion of the generated new segments within tube \mathbf{g} . This test needs to be added.

Appendix 2: Data for two examples in the paper

Example 1: Below we list all $\frac{\partial d_i}{\partial t_i}$ ($i = 0, 1, \dots, 19$) for the cube-curve g as shown in Figure 6:

$$\begin{aligned}
 d_{t_0} &= \frac{t_0}{\sqrt{t_0^2 + t_1^2 + 4}} + \frac{t_0 - t_{19}}{\sqrt{(t_0 - t_{19})^2 + 4}} \\
 d_{t_1} &= \frac{t_1}{\sqrt{t_0^2 + t_1^2 + 4}} + \frac{t_1 - t_2}{\sqrt{(t_1 - t_2)^2 + 5}} \\
 d_{t_2} &= \frac{t_2 - t_1}{\sqrt{(t_2 - t_1)^2 + 5}} + \frac{t_2 - 1}{\sqrt{(t_2 - 1)^2 + (t_3 - 1)^2 + 4}} \\
 d_{t_3} &= \frac{t_3 - 1}{\sqrt{(t_2 - 1)^2 + (t_3 - 1)^2 + 4}} + \frac{t_3}{\sqrt{t_3^2 + t_4^2 + 4}} \\
 d_{t_4} &= \frac{t_4}{\sqrt{t_3^2 + t_4^2 + 4}} + \frac{t_4 - 1}{\sqrt{(t_4 - 1)^2 + t_5^2 + 4}} \\
 d_{t_5} &= \frac{t_5}{\sqrt{(t_4 - 1)^2 + t_5^2 + 4}} + \frac{t_5 - t_6}{\sqrt{(t_5 - t_6)^2 + 4}} \\
 d_{t_6} &= \frac{t_6 - t_5}{\sqrt{(t_6 - t_5)^2 + 4}} + \frac{t_6 - 1}{\sqrt{(t_6 - 1)^2 + t_7^2 + 4}} \\
 d_{t_7} &= \frac{t_7}{\sqrt{(t_6 - 1)^2 + t_7^2 + 4}} + \frac{t_7 - 1}{\sqrt{(t_7 - 1)^2 + t_8^2 + 4}} \\
 d_{t_8} &= \frac{t_8}{\sqrt{(t_7 - 1)^2 + t_8^2 + 4}} + \frac{t_8 - t_9}{\sqrt{(t_8 - t_9)^2 + 4}} \\
 d_{t_9} &= \frac{t_9 - t_8}{\sqrt{(t_9 - t_8)^2 + 4}} + \frac{t_9 - 1}{\sqrt{(t_9 - 1)^2 + t_{10}^2 + 4}} \\
 d_{t_{10}} &= \frac{t_{10}}{\sqrt{(t_9 - 1)^2 + t_{10}^2 + 4}} + \frac{t_{10} - 1}{\sqrt{(t_{10} - 1)^2 + (t_{11} - 1)^2 + 4}} \\
 d_{t_{11}} &= \frac{t_{11} - 1}{\sqrt{(t_{11} - 1)^2 + (t_{10} - 1)^2 + 4}} + \frac{t_{11}}{\sqrt{t_{11}^2 + t_{12}^2 + 1}} \\
 d_{t_{12}} &= \frac{t_{12}}{\sqrt{t_{11}^2 + t_{12}^2 + 1}} + \frac{t_{12} - t_{13}}{\sqrt{(t_{12} - t_{13})^2 + 4}} \\
 d_{t_{13}} &= \frac{t_{13} - t_{12}}{\sqrt{(t_{13} - t_{12})^2 + 4}} + \frac{t_{13} - 1}{\sqrt{(t_{13} - 1)^2 + (t_{14} - 1)^2 + 4}} \\
 d_{t_{14}} &= \frac{t_{14} - 1}{\sqrt{(t_{13} - 1)^2 + (t_{14} - 1)^2 + 4}} + \frac{t_{14}}{\sqrt{t_{14}^2 + (t_{15} - 1)^2 + 4}}
 \end{aligned}$$

$$d_{t_{15}} = \frac{t_{15} - 1}{\sqrt{t_{14}^2 + (t_{15} - 1)^2 + 4}} + \frac{t_{15} - t_{16}}{\sqrt{(t_{15} - t_{16})^2 + 16}}$$

$$d_{t_{16}} = \frac{t_{16} - t_{15}}{\sqrt{(t_{16} - t_{15})^2 + 16}} + \frac{t_{16} - t_{17}}{\sqrt{(t_{16} - t_{17})^2 + 4}}$$

$$d_{t_{17}} = \frac{t_{17} - t_{16}}{\sqrt{(t_{17} - t_{16})^2 + 4}} + \frac{t_{17}}{\sqrt{t_{17}^2 + (t_{18} - 1)^2 + 1}}$$

$$d_{t_{18}} = \frac{t_{18} - 1}{\sqrt{t_{17}^2 + (t_{18} - 1)^2 + 1}} + \frac{t_{18} - t_{19}}{\sqrt{(t_{18} - t_{19})^2 + 101}}$$

$$d_{t_{19}} = \frac{t_{19} - t_{18}}{\sqrt{(t_{19} - t_{18})^2 + 101}} + \frac{t_{19} - t_0}{\sqrt{(t_{19} - t_0)^2 + 4}}$$

Example 2: For the example of a non-first class cube curve of Figure 7 we obtain the following t values, using either the original rubberband algorithm, or its revised version (new Option 3).

| Critical edge | x_{i1} | y_{i1} | z_{i1} | x_{i2} | y_{i2} | z_{i2} | t_{i0} | \bar{t}_{i0} |
|---------------|----------|----------|----------|----------|----------|----------|----------|----------------|
| e_0 | 0.5 | 1 | -0.5 | 0.5 | 1 | 0.5 | 1 | 1 |
| e_1 | -0.5 | 1 | 0.5 | 0.5 | 1 | 0.5 | - | - |
| e_2 | -0.5 | 2 | 1.5 | 0.5 | 2 | 1.5 | 0.7574 | 0.7561 |
| e_3 | -0.5 | 3 | 1.5 | 0.5 | 3 | 1.5 | 0.5858 | 0.5837 |
| e_4 | -0.5 | 4 | 1.5 | 0.5 | 4 | 1.5 | 0.4142 | 0.4113 |
| e_5 | -0.5 | 5 | 1.5 | 0.5 | 5 | 1.5 | 0.2426 | 0.2388 |
| e_6 | -0.5 | 6 | 1.5 | 0.5 | 6 | 1.5 | - | - |
| e_7 | -0.5 | 6 | 1.5 | -0.5 | 6 | 2.5 | 1 | 0.9581 |
| e_8 | -0.5 | 6 | 2.5 | -0.5 | 7 | 2.5 | - | - |
| e_9 | -1.5 | 6 | 3.5 | -1.5 | 7 | 3.5 | 0 | 0.5 |
| e_{10} | -2.5 | 6 | 3.5 | -2.5 | 6 | 4.5 | - | - |
| e_{11} | -3.5 | 6 | 4.5 | -2.5 | 6 | 4.5 | - | - |
| e_{12} | -3.5 | 5 | 4.5 | -3.5 | 6 | 4.5 | - | - |
| e_{13} | -3.5 | 5 | 5.5 | -3.5 | 6 | 5.5 | 0.2612 | 0.5 |
| e_{14} | -4.5 | 5 | 5.5 | -3.5 | 5 | 5.5 | - | - |
| e_{15} | -4.5 | 5 | 6.5 | -3.5 | 5 | 6.5 | - | - |
| e_{16} | -3.5 | 4 | 6.5 | -3.5 | 5 | 6.5 | 1 | 1 |
| e_{17} | 1.5 | 4 | 6.5 | 1.5 | 5 | 6.5 | 0.5455 | 0.5455 |
| e_{18} | 1.5 | 4 | 0.5 | 2.5 | 4 | 0.5 | 0 | 0 |
| e_{19} | 1.5 | 1 | -0.5 | 1.5 | 1 | 0.5 | 1 | 1 |

Table 2. Coordinates of endpoints of critical edges in Figure 7 and final t values obtained from the original or the revised rubberband algorithm. $p(t_{9_0})p(t_{13_0})$ is not contained in tube \mathbf{g} (see also Figure 7). $p(\bar{t}_{9_0})p(\bar{t}_{13_0})$ is contained in the curve .